

広島大学学術情報リポジトリ
Hiroshima University Institutional Repository

Title	Stereoscopic measurement of a fluctuating free surface with discontinuities
Author(s)	Tsubaki, Ryota; Fujita, Ichiro
Citation	Measurement science & technology , 16 : 1894 - 1902
Issue Date	2005
DOI	10.1088/0957-0233/16/10/003
Self DOI	
URL	https://ir.lib.hiroshima-u.ac.jp/00034909
Right	(c) 2005 IOP Publishing, Ltd. All rights reserved.
Relation	



Stereoscopic measurement of a fluctuating free surface with discontinuities

Ryota Tsubaki† and Ichiro Fujita‡§

† Graduate School of Science and Technology, Kobe University, Rokkodai, Nada-Ku, Kobe 657-8501, Japan

‡ Department of Architecture and Civil Engineering, Kobe University, Rokkodai, Nada-Ku, Kobe 657-8501, Japan

Abstract. This paper presents a new innovative method for measuring two dimensional water surface configurations. This method uses a pair of sequential images captured by two high-resolution CCD cameras arranged in a stereo position. The idea of the method is to make the water colour white so that the instantaneous water surface appears like a solid surface with a clear pattern when an irregular pattern of light is projected onto it. It should be noted that this method is suitable to measure waves with small amplitude accurately and at the same time discontinuous surface robustly. At first, we explain the measurement principle and the experimental procedure for obtaining stereo images. Secondly, we examine the measurement accuracy by applying our technique to calibrated wavy plates. In the application of the technique to actual flow fields, we first measure surface waves and ripples generated in a shallow water box, and show that we can trace the propagation of small waves as small as 1mm. In another application, we measure periodic surface fluctuation generated at an asymmetric cavity installed in an open-channel flow, demonstrating robustness of the technique applicable even when a discontinuous surface with wave breaking is presented in the course of the measurement.

1. Introduction

Most of the geophysical flows in nature, such as those found in rivers, lakes and oceans, have free surfaces. The existence of a water surface is of great importance because of its effect on the biological and global environments. It is also well known that water surface fluctuations play an important roll in the gas transfer mechanism between gas and liquid phases. However, that mechanism has not been fully understood so far because of the difficulty in measuring two-dimensional surface with a large-deformation with a reasonable accuracy even in laboratory scale experiments. It is true that a large number of numerical models, including the VOF method[1], the Level-set method[2], the C-CUP method[3], or the MARS method[4], have been developed significantly to simulate water surface deformations. However, quantitative comparison with experimental results are rarely reported due to the difficulty in obtaining two-dimensional surface shape precisely. Therefore, it is desirable to develop an innovative technique for free surface measurements in order to improve the numerical models and also to understand more deeply the surface flow phenomenon.

The measurement methods for free surface fluctuation can be categorized threefold, i.e. single point measurements, line measurements and two-dimensional measurements. In the past, single point measurement methods have long been used both in laboratories and in the field. The problem with point measurement instruments is their incapability to detect wavelength or spatial information of surface configurations without some assumptions. However, this type of probe is robust in natural conditions and still widely used in the actual field. Another method utilizes a Laser Light Sheet (LLS) shed from a transparent bottom wall of a laboratory flume[5]. In this method a cross-sectional line between a LLS and the water surface can be detected by an image analysis technique and time variation of surface shape on the line is obtained along with the velocity fields within the LLS by Particle Image Velocimetry(PIV). With this method it is possible to estimate the influence of water surface fluctuations on the flow field beneath the interface. The main shortcoming of this technique is that the measurement volume is limited to a line segment and it is impossible to examine the two-dimensional spatial variation of the surface fluctuation. It should also be noted that serious measurement errors occur due to random light reflection when the surface is contaminated by air bubbles. This method is of course inapplicable to field conditions.

The two-dimensional method belongs to the final category of surface measurement techniques. This method is classified into two subcategories: a method that uses one camera and another with two or more cameras. In the case of one camera, Tanaka *et al* [6] used speckle patterns generated by the refraction of uniform light at an air-water interface and provided information on the water surface shape or local slope of the water surface. Dabiri[7] and Dabiri and Ghrib[8] measured free-surface fluctuation by using a free-surface gradient detector(FSGD). The principle behind the FSGD is to colour code the different slopes of the free surface with different colours in order to establish a one-to-one correspondence between colour and slope. Zhang[9] measured short wind

waves using an FSGD-like technique, though not using a colour palette but gray scale distributions. However, these methods require complicated calibration processes and have the drawback of being incapable of measuring steep slope or discrete surfaces such as breaking waves(e.g. The maximum elevation measured by the FSGD method is 1.4mm). As compared with the aforementioned techniques, the new method presented herein is robust in the sense that it can measure three-dimensional surface configurations directly from a stereoscopic arrangement of two CCD cameras with a high resolution, even when the water surface has considerable irregularities with breaking, such as in a hydraulic jump.

2. Principle of measurement

The basic concept of stereoscopic measurements is the comparison of two or more images of the same location viewed from different angles at the same time. The two important procedures for the stereoscopic measurement are first to calibrate the camera parameters as accurately as possible and second to match the target points in each image as close as possible. In the present situation for measuring water surface shape, the second procedure is difficult to perform because the rays that go through the water surface are reflected and refracted so the pathway of the light changes depending on viewing location; therefore the pattern matching does not always yield a successful result due to the deficiency of appropriate image matching. In order to solve this problem, we mix a certain amount of white dye into the water and make the water colour white so that the entire water volume diffuses the light in immediate proximity to the water surface. The diffused light can be seen from every angle so it's easy to match images, but the reflected rays follow one certain pathway only, so are difficult or impossible to match. Therefore, we project an irregular model pattern onto the water surface by using an LCD projector. By the combination of the use of white-coloured water and the projection of a vivid pattern, the water surface motion can be seen as analogous to the motion of a waving flag when viewed from above the water surface. Note that the projected pattern itself is not used to measuring process directly but to do the pattern matching process adequately. This means we can measure surface profiles even when the projected pattern is distorted. Only with this experimental setup it would become possible to measure water surface configurations with a reasonable accuracy. In the experiments, to be presented in the following sections, we used two high resolution CCD cameras (KP-F100s , Hitachi Denshi co.) with a spatial resolution of 1304 by 1024 pixels and a temporal resolution of 12 frames per second. Each pixel of the CCD camera has 8bit gray scale information. One hundred and fifty images can be captured consecutively with this system. For illuminating the water surface, we use an LCD projector (VPL-CS4, SONY). The resolution of this projector is 800 pixels by 600 pixels, the brightness is 1000 ANSI(Lumens). The projected pattern is shown in figure 1. This irregular pattern is designed to maximize the accuracy of the pattern matching based on the cross-correlation technique. The appropriate amount of irregularities and

the uniformity of luminance are essential to obtain highly accurate matching results. To reduce redundant random reflection, the region surrounding the measuring area is masked with black paper. The LCD projector is set about one metre above the water surface for a better illumination of the irregular pattern. We use a conventional camera model, equation 1 and 2, to establish a transformation relationship between the physical coordinates (X, Y, Z) and the screen coordinates (x, y) . The camera parameters to determine are the camera location (X_0, Y_0, Z_0) , the viewing angle $(\omega, \varphi, \kappa)$, the focal length c , and the lens distortion parameter D (see figure 2).

$$x = -c \frac{a_{11}(X - X_0) + a_{12}(Y - Y_0) + a_{13}(Z - Z_0)}{a_{31}(X - X_0) + a_{32}(Y - Y_0) + a_{33}(Z - Z_0)} + \delta x \quad (1)$$

$$y = -c \frac{a_{21}(X - X_0) + a_{22}(Y - Y_0) + a_{23}(Z - Z_0)}{a_{31}(X - X_0) + a_{32}(Y - Y_0) + a_{33}(Z - Z_0)} + \delta y \quad (2)$$

$$\begin{pmatrix} a_{11} & a_{12} & a_{13} \\ a_{21} & a_{22} & a_{23} \\ a_{31} & a_{32} & a_{33} \end{pmatrix} = \begin{pmatrix} 1 & 0 & 0 \\ 0 & \cos \omega & \sin \omega \\ 0 & -\sin \omega & \cos \omega \end{pmatrix} \begin{pmatrix} \cos \varphi & 0 & -\sin \varphi \\ 0 & 1 & 0 \\ \sin \varphi & 0 & \cos \varphi \end{pmatrix} \begin{pmatrix} \cos \kappa & -\sin \kappa & 0 \\ \sin \kappa & \cos \kappa & 0 \\ 0 & 0 & 1 \end{pmatrix} \quad (3)$$

$$\delta x = Dr^2x \quad (4)$$

$$\delta y = Dr^2y \quad (5)$$

$$r = \sqrt{x^2 + y^2}$$

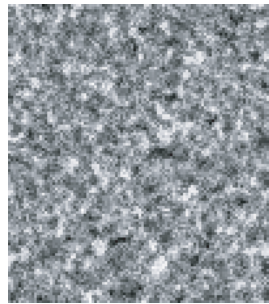


Figure 1. Projected pattern

Here, we assume that the origin of the screen coordinate (x_0, y_0) is located at the centre of the screen coordinates. The other seven coefficients are determined by the least square method using a calibration plate or points. The set of coefficients are calculated for each camera through the abovementioned calibration procedure and used for the 3-D surface measurements.

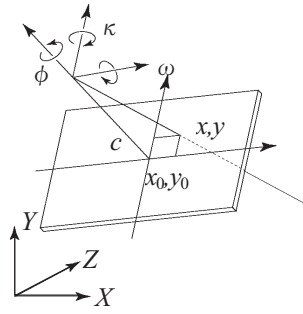


Figure 2. Geometry of coordination

To reconstruct a water surface shape from a pair of images, we have to find in each image the corresponding points for the same physical point. In this study, we use the following procedures to find the matching points efficiently. Let's call one of the CCD cameras the first camera and its image the first image, and the image of the second camera the second image. In the first place, we divide the area of the first image into rectangular segments. By substituting the coordinates of the centre of the segment, say (x_s, y_s) , into equation (1) and (2), we can establish a line passing through the centre of the segment in the physical space. The line can be expressed by the following equation.

$$\frac{X - \beta_1}{\gamma_1} = \frac{Y - \beta_2}{\gamma_2} = \frac{Z - \beta_3}{\gamma_3} \quad (6)$$

where β_s and γ_s ($s = 1, 2, 3$) are constant values. Since we know that the variation of water surface level is limited to a certain range, we can assume a candidate point (X_C, Y_C, Z_C) for a water surface within the range on this epipolar line. Then by the substitution of these coordinates into equations 1 and 2 for the second image, candidate coordinates in the second image (x_c, y_c) can be obtained. If the local image, or the template, around the point (x_s, y_s) is the same as or similar to the image around the candidate point (x_c, y_c) , the matching would be successful and we can say that the candidate point lies on the water surface. However, this situation cannot occur in general, so we have to find the most appropriate location so that the respective local images correspond to each other. As the method for searching for similarity between templates we utilize the cross-correlation technique with parabolic sub-pixel fitting, whose accuracy is considered to be about 0.1 pixels. The accuracy of sub pixel-fit is one of the main factors of resolution of this measurement. The distance between cameras and physical resolution of images are another key factor. So accuracy of measurements can be controlled by changing arrangements of equipment or improving resolution of images.

3. Experimental setup

The experimental setup for measurement is shown in figure 3. To measure an 18cm by 14cm area, CCD cameras are set one metre from the target, and the distance between the

cameras is set to about 30cm to obtain a reasonable measurement accuracy and for valid pattern matching. To calibrate camera parameters, two plates glued perpendicularly (on which a 2.5cm pitch grid pattern is coated on each side of the plate) are used (figure 4). An example of the projected pattern on each plate is indicated in figure 4b.

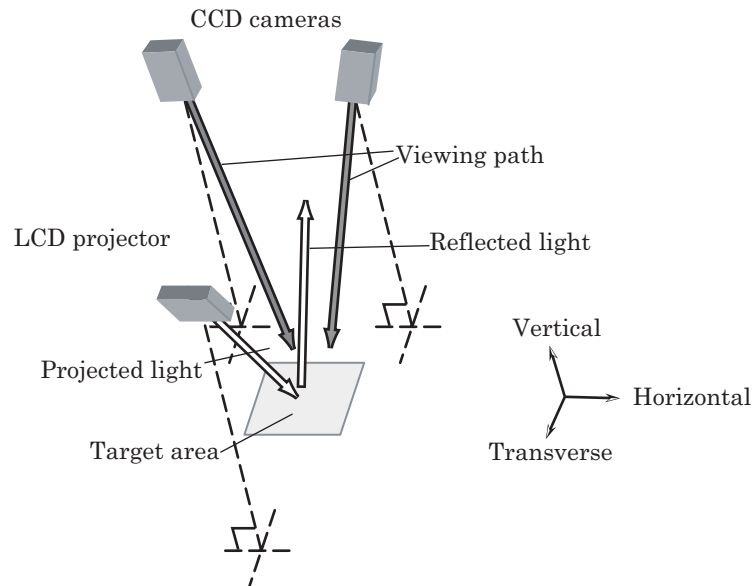


Figure 3. Experimental setup

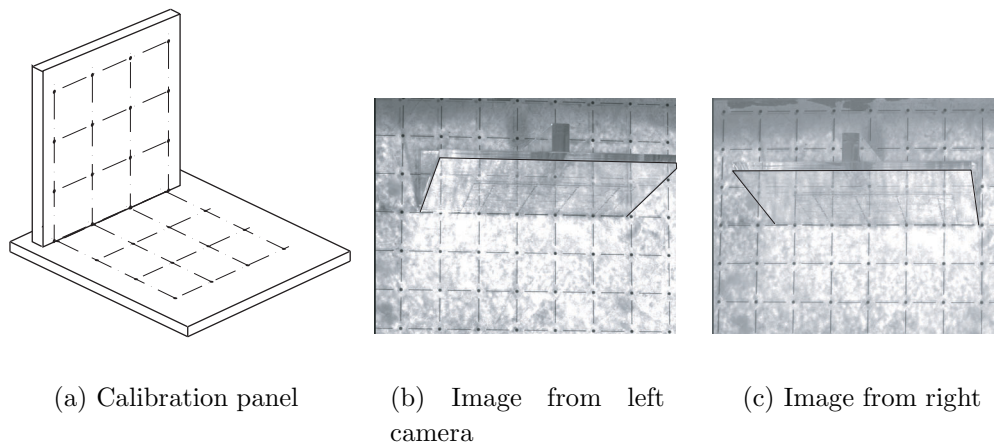


Figure 4. Calibration

3.1. Still water surface: for calibration

In the first place, a static water surface is measured in order to estimate the error in the system caused by mechanical or optical measurement errors. As mentioned previously,

the water is stained by white dye. The captured area is about 18cm by 14cm in the present configuration. The result is shown in figure 5(a). The measurement is performed at a spacing of about 0.6cm and within a height range between one and two centimeters. Although the result should yield a flat plane, the measured surface height distribution shows somewhat uneven results having a relatively small depth in the middle of the measurement area. However, since the error distribution seems to have a systematic tendency, it becomes possible to minimize the error and correct the result by using the following quadratic distribution function as a correction function.

$$z' = z + b_1x^2 + b_2x + b_3y^2 + b_4y + b_5 \quad (7)$$

where z' is the corrected height and b_1, b_2, \dots, b_5 are coefficients.

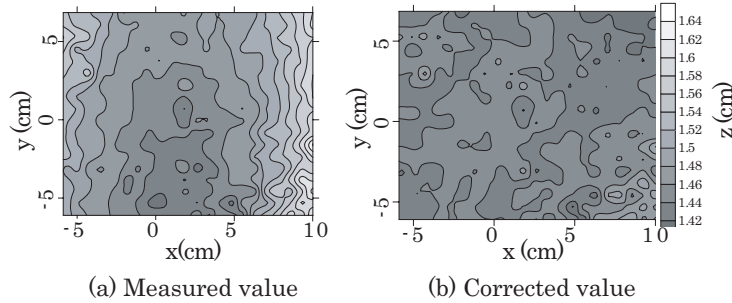


Figure 5. Still water surface

The result after the correction is shown in figure 5(b). The standard deviation of the surface height distribution is 0.015cm, which is sufficiently small for the measurement of water surface waves. Hereafter we use this correction procedure every time before we do the measurements.

4. Evaluation of measurement accuracy

To evaluate the measurement accuracy, several static targets with and without discontinuous surface are measured by using this method.

4.1. Human hand: thick object

We measure a human hand put in a flat plane (figure 6). The result is somewhat blurred and has some abnormal values in the discontinuous region between the hand and the plane, but the general form of the hand is well measured.

4.2. Hemisphere: object with steep slant shape

We measure a hemisphere made of Styrofoam with a diameter of 0.1m (figure 7). The measured result is shown in figures 8,9 and 10. The round shape around the top of

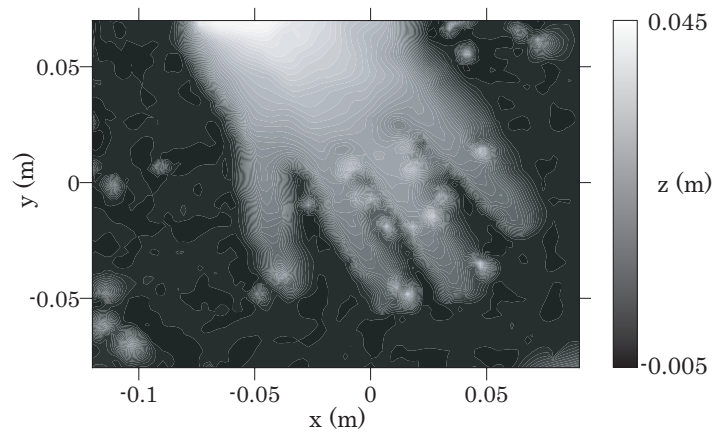


Figure 6. Shape of hand

the hemisphere is well measured. There is a blind side area in the $+y$ side of sphere because images are captured from the $-y$ direction. In this area, no values are measured. However, considering that the surface slope becomes almost vertical closer to the edge of the hemisphere, the new method successfully obtains the height of the hemisphere.

The standard deviation of error along both axes is about 0.8mm, which is acceptable for capturing general shape of the hemisphere.

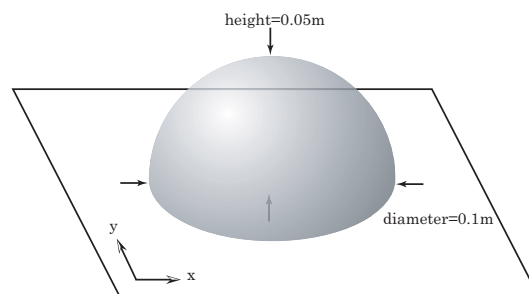


Figure 7. Configuration of hemisphere

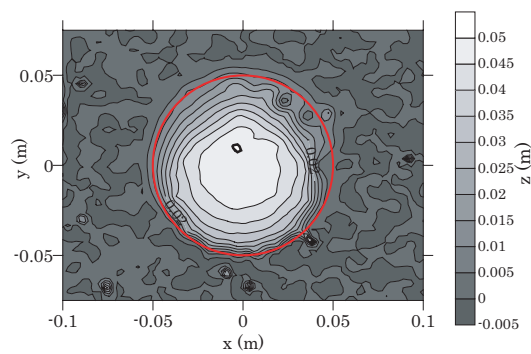


Figure 8. Height distribution

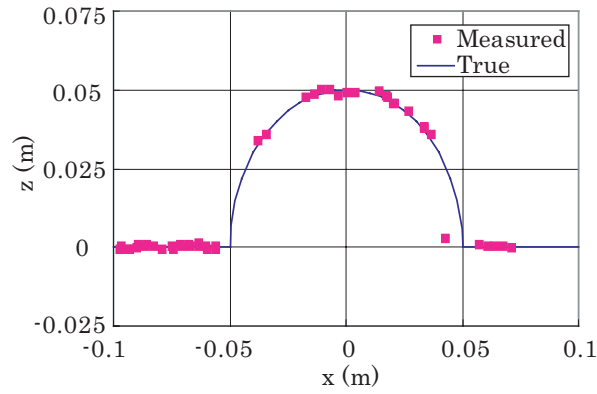


Figure 9. Height variation along x axis

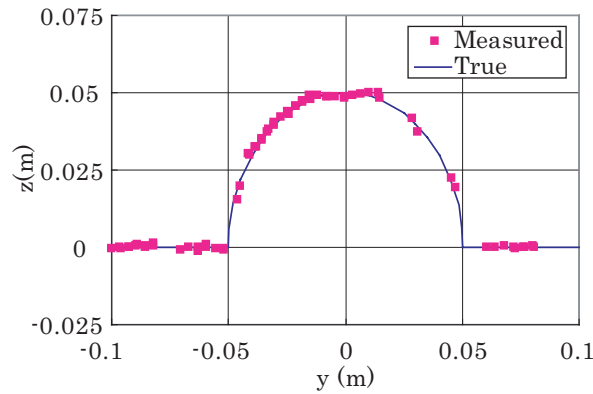


Figure 10. Height variation along y axis

4.3. Wavy plate: continuous roughness

A ribbed polyvinyl chloride board is measured to estimate measuring accuracy for the corrugated shapes that are seen in natural wave fields. The amplitude is 0.008m and the wavelength is 0.0323m.

The planar height distribution is shown in figure 11. The ribbed shape, amplitude and wavelength are well measured. In figure 12, the measured result is compared with the measured value by another precise method (using a coordinate measuring machine with accuracy of $1\mu\text{m}$). The measured values by the present method have a margin of error of about 10% but the smoothed result shows good agreement to a precise value.

5. Measurement of moving targets

To evaluate the measurement accuracy for moving targets, propagating one-dimensional and two-dimensional waves are measured.

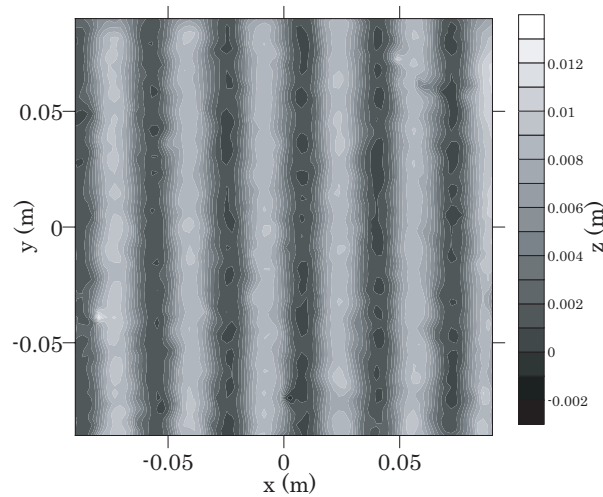


Figure 11. Contours of measured height

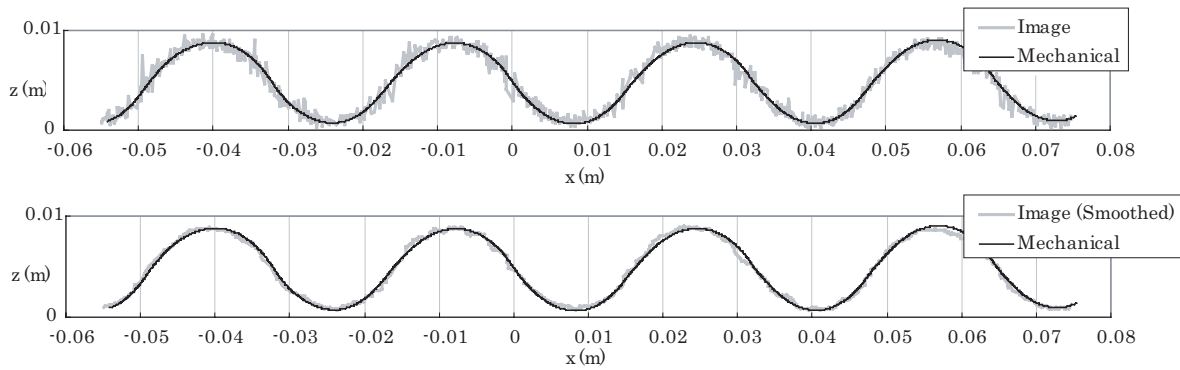


Figure 12. Height variation along x axis on $y=0$. Top plot shows measured value and bottom plot shows moving averaged result

5.1. One-dimensional wave

Using the same shallow box as in the case of still water surface measurements, a wave is generated by uplifting one side of the box. The generated wave reflects at both sides of the channel and finally fades away. The height of the wave is about 0.5cm at first. One sequence of measured results for a local area of 13cm by 17cm is shown in figure 13 and 14. One-sixth seconds passes between each figure. The wave is generated by fluctuating the minus side of the x-axis. The result shows propagation of the gravity wave with a reasonable accuracy.

5.2. Propagation of wave rings

Here, wave rings generated by dropping small droplets are measured. Figure 15(a) shows the measurement results. The wave spreading in a circular pattern is captured well, but

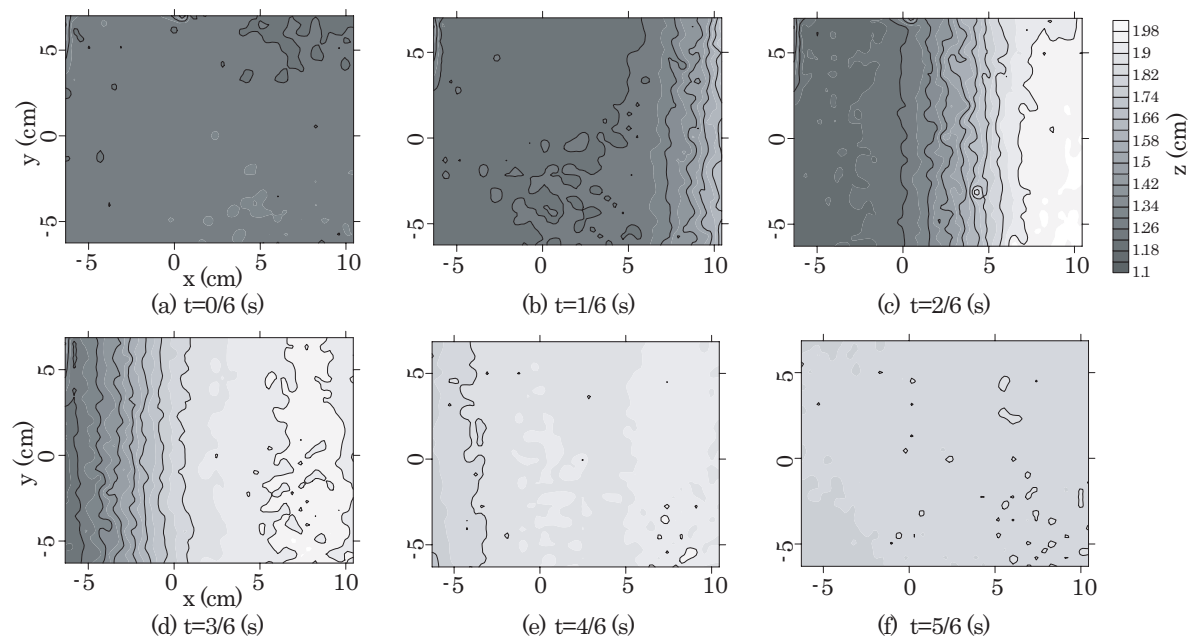


Figure 13. Propagating wave

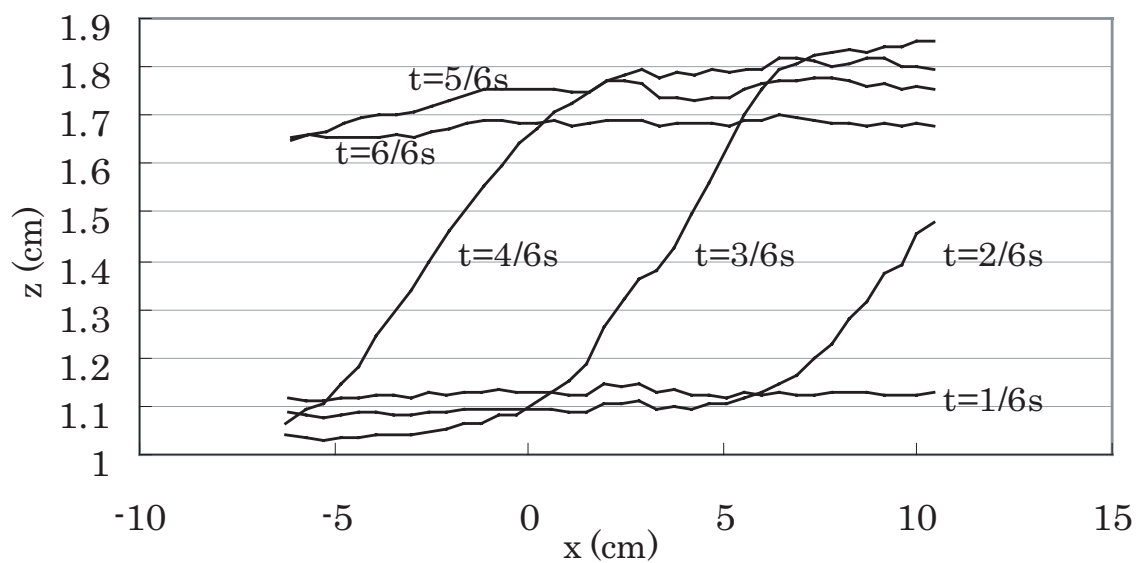


Figure 14. Propagating wave (Cross section of $y=0$)

a fluctuation of small amplitude is seen in the whole area. In the caribration process previously explained in section 3.1, the standard deviation of the measurement values for the flat water surface was 0.015cm , which is approximatly 16% of wave height (0.1cm) in the present case. Whereas, the propagation of the wave can be seen more clearly in the moving averaged result (figure 15(b)). In this method, increasing the number of measure points is easy (up to image resolution) so adequate filtering for large number of the data can also boost accuracy of measurement

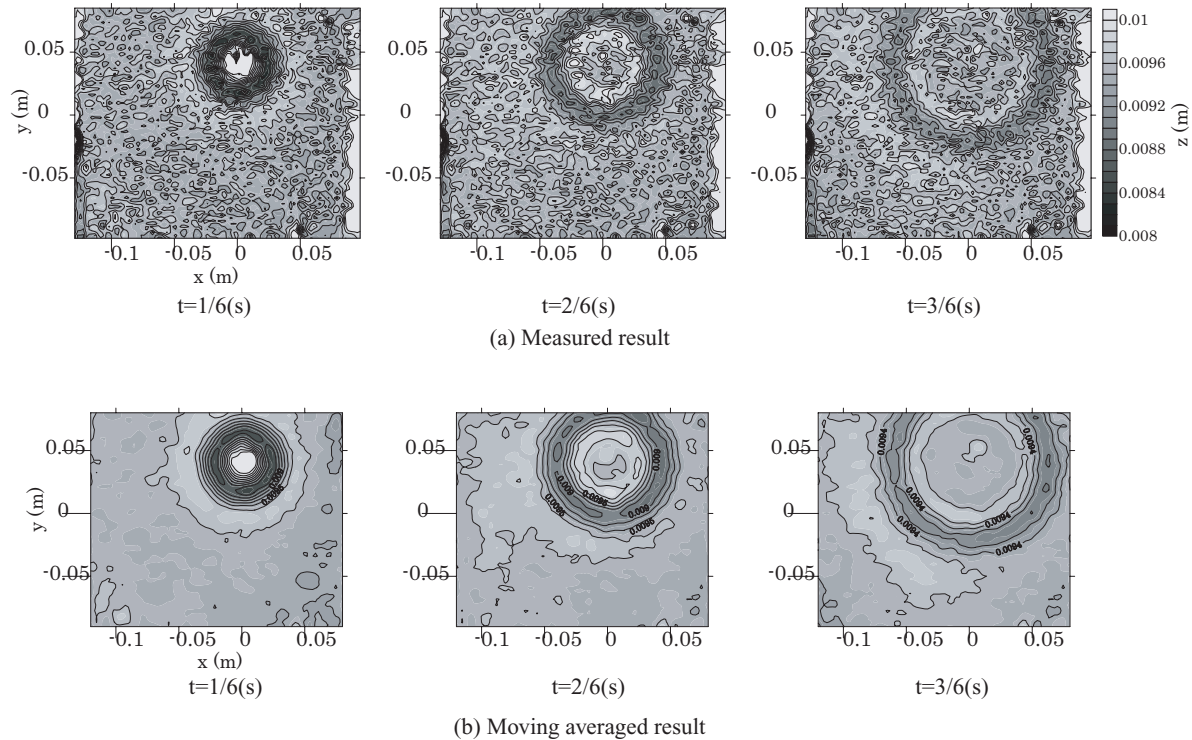


Figure 15. Propagating wave ring

6. Measurement of flow over an asymmetric trench: flow with a hydraulic jump

As an application of the method to a critical situation in which three-dimensional measurement is usually difficult to perform, we try to measure breaking waves with complicated water surface shape. Fujita[10] reported that, even in a steady open channel flow, an oscillating hydraulic jump could occur at an asymmetrical trench installed in an open channel for a specific hydraulic condition. Fujita measured two-dimensional velocity distribution by PTV (particle tracking velocimetry) within an LLS shed upward from the channel bottom. However with this method, the LLS is randomly deflected at the water surface due to small air bubbles generated by wave breaking and thus the clear interface between air and water is not captured successfully. In this study, by using the same channel as used by Fujita, time-dependant water surface variations are

measured to examine the applicability of the method. The channel width used for the experiment is 0.15m and its length is 6.0m. The asymmetrical trench, with a relative height difference of 1cm and a length of 8cm, is set in the middle of the channel as shown in figure 16. The coordinate system is schematically indicated in figure 17. The downstream boundary condition is the free outfall condition without any control. The quantity of flow discharge is $0.00075m^3/s$ and the channel slope is 1/500. The flow over the downstream face of the step plunges down and induces a hydraulic jump. After that the flow hit the forward facing step and the water surface rise, like a standing wave. The swell of the surface oscillates periodically under the above hydraulic condition with a period, T , of 1.75 seconds. The surface is disturbed by wave breaking, so several rays reflected by the chaotic surface go to the CCD cameras directly and the trajectory of these reflected rays makes bright hair-like noise as shown in figure 18(a). The noise has a distinctive trend so can be removed well using a filtering procedure (figure 18(b)).

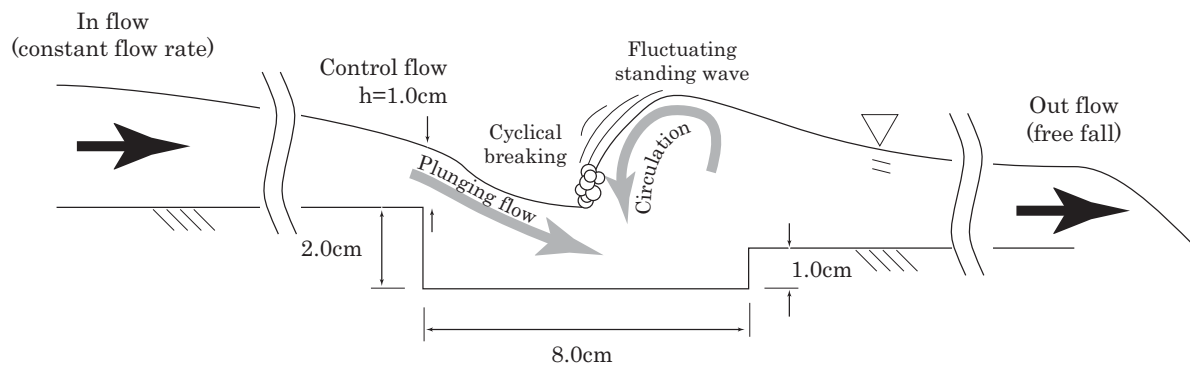


Figure 16. Assymetrical trench

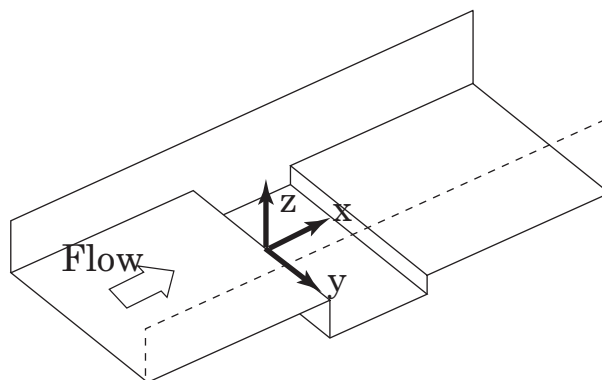


Figure 17. The coordinate system

Typical surface flow patterns during one period are shown in figure 19. At the moment $t=0$, the supercritical flow extends down to the region $x < 3cm$, showing the smooth water surface within this region, while in the downstream region the water surface displays an apparent irregular pattern. This irregularity is generated just after

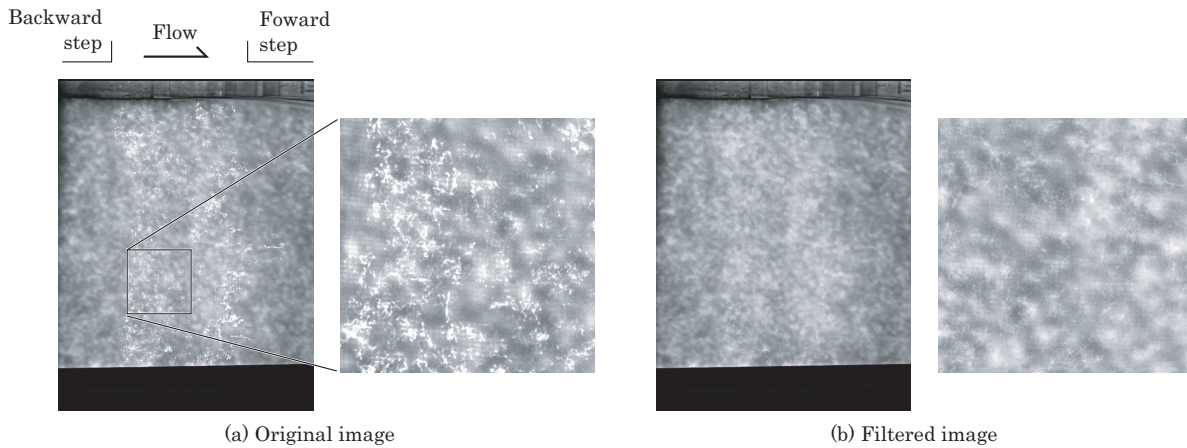


Figure 18. Reflection noise. Low-pass filter removes bright hair-like noise well

the breaking of a weak hydraulic jump towards the upstream direction. The new method clearly captures the boundary between the two regions. At $t=0.19T$ ($=2/6s$), the supercritical region extends farther in the downstream direction and the water surface begins to rise locally at the downstream end of the trench section. The protrusion observed in the centre of the channel is caused by the matching error of local surface images, which can be easily eliminated by a statistical procedure. At the subsequent moments $t=0.38T$ ($=4/6s$) and $t=0.57T$ ($=6/6s$), the water level shows a sudden increase at the downstream end of the trench section. The protrusion in the figure is again a matching error. As can be observed in the figure at $t=0.57T$ ($=6/6s$), the water surface demonstrates three bumps in the span wise direction. These surface bumps are also clearly observed by a visual inspection, which suggests that the structure of the flow at the section changes drastically from a nearly two-dimensional one to a well-defined three-dimensional structure as a result of the impingement of the supercritical flow on the rear end of the trench section. After the bumps reach a critical situation, they begin to break down towards the upstream direction as shown in figure 19 at $t=0.76T$ ($=8/6s$). Finally at $t=0.86T$ ($=9/6s$), the breaking waves cease to show a strong three-dimensional structure and prepare for the next periodic cycle. As has been demonstrated in the sequential results shown in figure 19, the new measurement method is shown to be successful in measuring the complicated open channel flow that accompanies large surface deformation.

7. Conclusion

We developed a new method for measuring two-dimensional water surface variations. After we examined the accuracy of the method by applying it to a calibration plate, we measured several objects and the waves generated in a shallow box. Then, we measured the periodic surface oscillation with breaking produced at an asymmetric open-channel trench and showed that the presented method has a large dynamic range and is capable

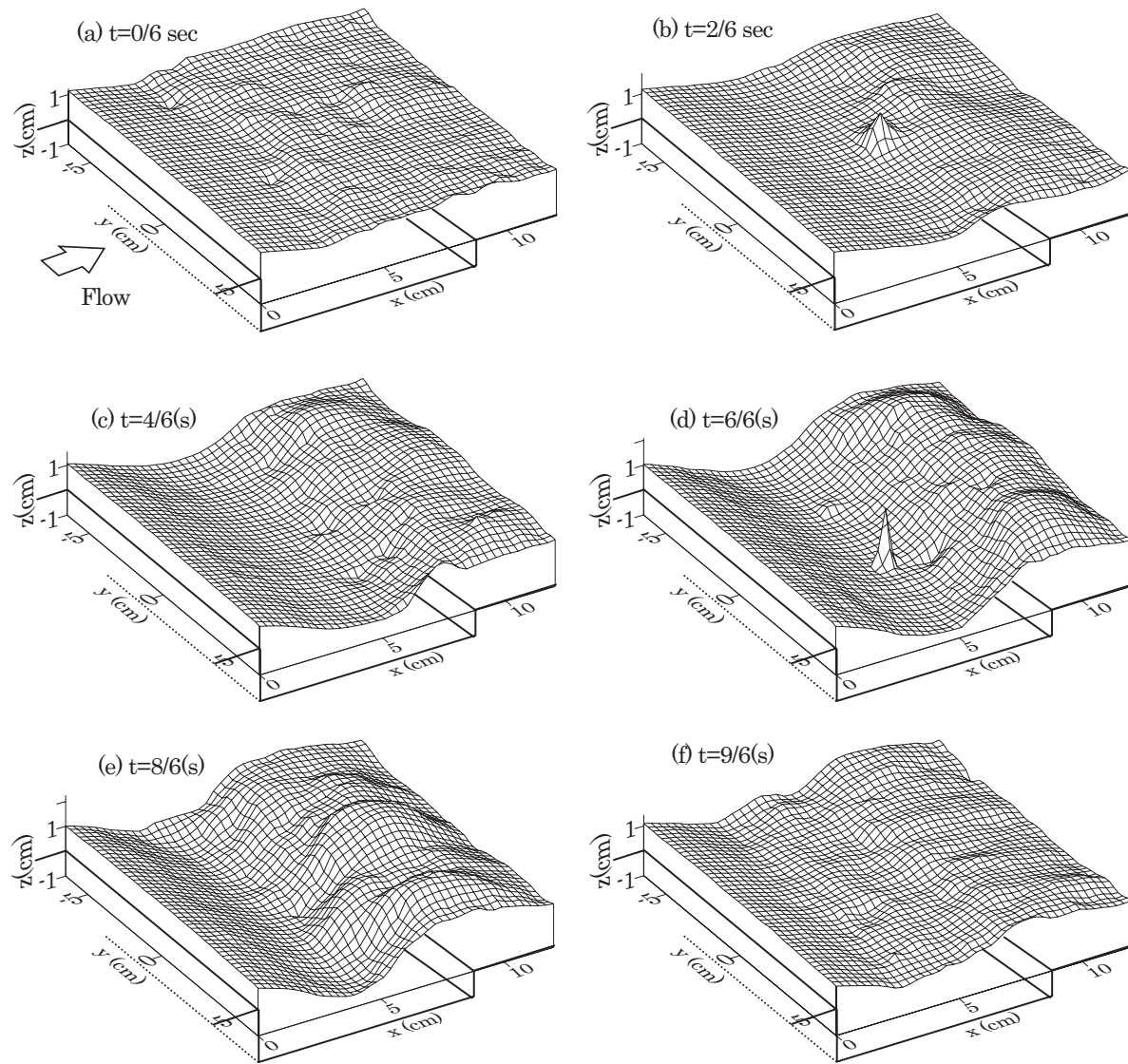


Figure 19. Measured result

of obtaining water surface variations even for the cases in which conventional methods are not applicable. The shortcoming of the current measurement system is its low temporal resolution of 12 fps. However, this can be overcome by using a set of high-speed video cameras. To the best of our knowledge, only with the use of the new method, it becomes possible to measure the three-dimensional deformation of the wave including breaking. The information obtained by this method would be essential to evaluate the accuracy of the three-dimensional numerical simulation models.

Acknowledgement

The authors are deeply grateful to Dr. Jeremy D. Bricker of the Kobe University.

References

- [1] Hirt C W and Nichols B D 1993 Volume of Fluid (VOF) Method for the dynamics of Free Boundaries *J. Comput. Phys.* **62** 1865-71
- [2] Osher S and Sethian J A 1988 Fronts Propagating with Curvature-Dependent Speed: Algorithm based on Hamilton-Jacobi Formulation *J. Comput. Phys.* **79** 12-49
- [3] Yabe T and Wang P Y 1991 Unified Numerical Procedure for Compressible and Incompressible Fluid *J. Phys. Soc. Japan* **60** 2105-8
- [4] Kunugi T, Satake S and Ose Y 1999 Direct Numerical Simulation of Turbulent Free-Surface Flow *Turbulence and Shear Flow Phenomena-1* (Begell House Inc.) 621-26
- [5] Miyamoto H and Shimoyama K 2004 Experimental study on influence range of water surface fluctuations in turbulent open-channel flows *Proc. Int. Conf. on Hydrosience and Engineering on CD-ROM*
- [6] Tanaka G, Bi W-T, Sugii Y, Okamoto K and Madarame H 2002 Stereoscopic PIV Combined with Specklegram Method Applied for Simultaneous Measurements on Free Surface Turbulence *Proc. of 10th Int'l Symp. on Flow Visualization* paper number 141
- [7] Dabiri D 2003 On the interaction of a vertical shear layer with a free surface *J. Fluid Mech.* **480** 217-32
- [8] Dabiri D, Ghrib M 2001 Simultaneous free-surface deformation and near-surface velocity measurements *Exp. Fluids* **30** 381-90
- [9] Zhang X 2003 Surface image velocimetry for measuring short wind wave kinetics *Exp. Fluids* **35** 653-65
- [10] Fujita I 2002 Particle Image Analysis of Open-channel Flow at a Backward Facing Step Having a Trench *Journal of Visualization* **5** 4 335-42